Available online at www.sciencedirect.com

ScienceDirect

Energy Procedia 77 (2015) 321 – 330

Energy Procedia

5th International Conference on Silicon Photovoltaics, SiliconPV 2015

Electronic properties of Al p^+ surfaces formed by laser doping from aluminium oxide precursors: implications for PERC cell design and performance

Daniel Walter[a], Andreas Fell[a], Marco Ernst[a], Evan Franklin[a], Klaus Weber[a]

[a] *Centre for Sustainable Energy Systems, Australian National University, Canberra, ACT, 2601, Australia*

Abstract

Aluminium oxide (Al_2O_3) functions doubly as a high-quality surface passivation material for crystalline silicon and as an aluminium (Al) p-type precursor for laser doping. Thus, p^+ doping based on laser ablation of Al_2O_3 thin-films deposited on a silicon substrate is an attractively simplified process for concurrent local contact definition and aligned surface doping. A number of studies have demonstrated this process, but a careful examination of the influence of laser parameters on the electronic properties of the Al laser doped p^+ surface itself, including the influence of post-doping annealing, has yet to be presented. Such information is valuable for establishing process windows and for providing parameters by which the contact geometry can be optimized and the performance of locally Al_2O_3 laser doped solar cells predicted. In this work, we present accurate characterization of the electronic properties of primary importance to solar cell performance: effective surface recombination and contact resistivity. Recombination at the Al_2O_3 laser doped p^+ surface is found to exceed that of equivalently-doped p^+ silicon from furnace diffused boron, while contact resistivity to vacuum evaporated Al is up to two orders of magnitude less than screen-printed, fired Al. Based on this characterization, computer simulations demonstrate that with optimized rear contact geometries, an industrially relevant PERC cell can approach 21 % efficiency, and the high-performance UNSW PERL structure can exceed 24 %.

Peer review by the scientific conference committee of SiliconPV 2015 under responsibility of PSE AG

Keywords: laser doping; aluminium oxide

Peer review by the scientific conference committee of SiliconPV 2015 under responsibility of PSE AG

doi:10.1016/j.egypro.2015.07.046

1. Introduction

Focused laser irradiation is a well-established tool for locally doping the near-surface region of silicon substrates and solar cells [1,2] The laser energy simultaneously ablates surfaces films, forming a vapour, and locally melts the near-surface region of the silicon substrate, into which the vaporised elements can diffuse. In this fashion, surface films containing silicon dopant elements can act as precursors for n- and p-type doping. Concurrent ablation and doping is ideally suited for aligned local contact openings and back-surface field (BSF) or emitter formation, and in recent years several studies have demonstrated locally laser doped contact openings in high efficiency cell structures [3–6].

A major limitation of laser doping, however, is the requirement for customised or additional surface layers to provide the dopant element. Examples include the doping of conventional passivating dielectric films such as silicon nitride [7,8], or the deposition of dopant-specific films, such as phosphoric acid [9]. These approaches complicate processing by requiring an additional or customised deposition and/or the subsequent removal of the precursor residual.

Aluminium oxide (Al_2O_3) potentially avoids such complications by functioning both as a high quality surface passivation material for p-type silicon [10] and a rich source of aluminium (Al), a p-type dopant in silicon [11]. Laser doping from Al_2O_3 thus requires no customisation of the dielectric, and avoids post-doping removal. Previous work has described p-type doping of silicon from Al_2O_3 dielectrics using a range a laser wavelengths, from the ultraviolet [12] to the infrared [4,11,13], and pulse lengths from pico [14] to microseconds [4]. Al_2O_3 and typical SiN capping layers are both transparent throughout the near UV, optical and infrared wavelengths, and we can therefore expect the laser wavelength to have a minimal influence on the doping process. However, the laser pulse length may influence laser damage by changing the instantaneous pulse energy, the duration of the melt cycle and the corresponding recrystallization velocity.

Where recombination has been measured directly, the general consensus is that Al_2O_3 laser doped (Al_2O_3-LD) silicon is more recombination active than would be expected from the equivalent doping density of boron or fired aluminium[*]. Values ranging from approximately 4,500 fA cm^{-2} [11] to 30,000 fA cm^{-2} [13] have been quoted for Al-LD silicon from a range of Al_2O_3 dielectric configurations[†]. The wide range of values may be the influence of dielectric capping layers and/or the variable temporal laser pulse lengths. Laser damage itself has been attributed to crystalline defects formed during melt re-solidification, which may accumulate with the number of melt cycles, or to thermal stresses between the substrate and dielectric films [21,22]. These factors may not be specific to laser doping from Al_2O_3 itself, and it is also possible that there is a contribution to recombination from Al-O complexes, which have been implicated in increased recombination in Al doped silicon formed by non-laser doping [23–25]. Al_2O_3 is of course rich in aluminium and oxygen, both of which are incorporated into the laser-induced silicon melt at high concentrations.

Two approaches have been presented to reduce recombination in Al_2O_3-LD silicon using pulsed laser irradiation. The first involves doping from a dielectric stack of an intermediate Al_2O_3 layer and a boron-rich silicon carbide capping layer, thereby over-doping Al with boron [4]. This approach has demonstrated a marginal reduction in recombination ($j_0 \approx 4{,}000$ fA cm^{-2}), and was implemented for rear contact openings on small-area PERC cells with efficiencies of 21.4 %. It also indirectly demonstrates a dilemma of laser processing Al_2O_3 passivated surfaces: a potentially unavoidable increase in recombination as a result of the indiscriminate inclusion of the elements present in the dielectric. The second approach proposes annealing the laser doped silicon in the presence of hydrogen, which may be sourced either from the surface dielectrics or the ambient atmosphere (e.g. forming gas) to passivate the laser induced defects [26]. In this case, post-annealing increases in implied V_{oc} on laser doped test structures were

---

[*] The exception is the work of *Harder et al* [15], who use the slope of the high-injection inverse lifetime curve described by *Kane & Swanson* [16] to measure recombination at Al_2O_3 LD silicon equivalent to that of furnace-diffused boron . However, this characterisation method is prone to understatement at high values of j_0 where the surface carrier concentration strongly deviates from the average value, as observed by several studies [17–19] and the original authors themselves [16].

[†] In the literature recombination is often extracted usi ng the Fischer method [20] and reported as an effective surface recombination velocity, S_{eff}. For comparison to the data presented in this study, S_{eff} was converted to j_0 using the relationship $j_0 = S_{eff} q n_i^2/(N + dn)$.

reported, but quantification of the recombination properties themselves were not. This recovery is also general to laser processed silicon, as demonstrated for other laser-doped silicon [27].

In the context of previous work, the outstanding question is to what extent laser doping from Al_2O_3 dielectric layers, which results in relatively high contact recombination, is compatible with high efficiency solar cells. Accurate quantification of the key electronic parameters of Al_2O_3-LD – minority carrier recombination and contact resistivity – would facilitate cell simulations and optimisation and define process windows. Thus, this work presents a careful characterisation of recombination and contact resistivity of Al_2O_3-LD silicon across a range of laser parameters for a 532 nm, nanosecond pulse length laser. We perform doping from single layer Al_2O_3 and from an industrially relevant Al_2O_3/SiN dielectric stack in order to expose the influence of the SiN capping layer, which has been correlated with increased recombination at laser-doped silicon [21]. We measured the response of recombination to post-doping annealing in ambient and forming gas atmospheres. Contact resistivity was measured to vacuum evaporated aluminium. With this information, three-dimensional numerical computer simulations are used to predict the efficiency potential of an industrially typical PERC cell and the record-efficiency UNSW PERL cell [28] when these structures are modified to incorporate rear-surface Al_2O_3 passivation and Al_2O_3 laser doping. In doing so, we provide an indication of efficiency potential in current industrial cell technologies, in addition to a device in which the Al_2O_3-LD contacts will be a primary source of recombination.

2. Experimental details

Laser doping was performed using an *Innolas* 532 nm, nanosecond pulse-length laser system. The laser repetition rate was 100 kHz, for which the full-width half maximum pulse length was approximately 48 ns. The laser scan speed was varied to produce spatial pulse overlaps of 30, 50 and 90 %, which increases the number of melt cycles in the near-surface region of the silicon substrate. Pulse energy was varied from the threshold of ablation of the dielectric film, through to the threshold of ablation of the silicon substrate. These thresholds were determined using light microscope images of the laser-processed substrate, and determined from the first visual evidence of dielectric removal through to clear ablation of the silicon substrate. As a result, the thresholds are only approximate and some silicon ablation is possible at the intermediate pulse energies. Across this energy range, the pulse diameter ranged from approximately 13 – 22 μm, as determined by optical microscopy.

The Al_2O_3 films were deposited as both a single layer and as the intermediate layer in an Al_2O_3/SiN stack on p-type, (100), 200 Ω-cm, chemically-polished float-zone, 300 μm-thick silicon substrates. The Al_2O_3 films were deposited with an Oxford Instruments Flex-Al system with a thickness of approximately 20 nm. Capping layers of SiN were deposited using a *Roth & Rau* SiNA inline PECVD system. The Al_2O_3 passivation was activated with a 15 minute anneal at 425 °C in ambient conditions on a hotplate. The SiN thickness was approximately 80 nm, with a refractive index of 2.05 at 632 nm. These dielectrics are of course highly transparent in the optical wavelengths, and will therefore be ablated indirectly by the 532 nm laser, via thermal transfer from the silicon substrate and at higher energies by the ablation of the silicon itself.

For both dielectric configurations, two sets of each laser parameter were processed. Each set of parameters then received different post-doping thermal treatments. One was annealed on a hotplate in ambient conditions at increasing temperatures of 250, 350 and 450 °C, each for 30 minutes. The other sample received a single anneal at 450 °C in forming gas (2 % H_2 in N_2) for 30 minutes. For the hotplate anneal, a source of hydrogen was available in the dielectric films themselves. The Al_2O_3 film has a hydrogen concentration of approximately 1 – 2 % (atomic percentage) [10], and the SiN film has a concentration of 15 – 20 % [29]. Once doped and ablated, no further depositions were performed and the measured recombination is for doped, un-metallised and un-passivated silicon.

Recombination at the Al_2O_3-LD surface was measured via luminescence-coupled numerical device simulations in *Quokka* [30], which is described in detail in [31]. This technique uses electronic and luminescence models of test structures to numerically fit recombination at Al_2O_3-LD lines to measured luminescence signals of the test structures. Uncertainty in the extracted recombination was determined by the standard deviation of the output of 100 Monte Carlo simulations for three input parameters. The laser line width, luminescence signal and luminescence calibration factor were treated as normally distributed variables with a standard deviation reflecting the approximate measurement uncertainty. The steady-state photoluminescence signal of the test structures was measured via

photoluminescence imaging before and after annealing. A reference region was left unprocessed on each sample to ensure that the annealing step did not alter recombination at the undoped, Al_2O_3-passivated surfaces.

In this work, recombination is parameterised by j_0, the recombination current prefactor, in units of fA cm^{-2}. The use of this term follows the recent prescription of *Cuevas et al* [32]. It is also referred to in the literature variously as the reverse saturation current density and the dark current density, among other terms.

Contact resistivity was measured with the transfer length method [33]. The Al_2O_3-LD process was extended to continuously dope areas measuring 22 × 5 mm^2, with consistent pulse overlap in the x and y directions. Two sets of parameters were again processed, with one set receiving a brief, 30 s etch in 1 % (by volume) aqueous hydrofluoric (HF) acid solution. The samples were then metallised by vacuum evaporated aluminium in an *Applied Materials* ATON 500 inline evaporator. The aluminium thickness was approximately 2 µm. The un-etched samples were then sintered on a hotplate for 30 minutes at both 250 and 350 °C.

Sheet resistance was measured using four-point probe on continuously doped square features measuring 10 x 10 mm^2 on high resistivity p-type substrates.

3. Results and discussion

3.1. Recombination

Prior to annealing, recombination at the Al_2O_3-LD surface for both dielectric configurations and all laser parameters exceeded 10,000 fA cm^{-2} (figure 1, top). Recombination decreases with increasing pulse energy, correlated with decreasing sheet resistance. However, increased pulse overlap measurably increases recombination. This observation is consistent with an accumulation of crystalline defects with an increasing number of melt cycles. The additional thermal cycles did not reduce sheet resistance, which is an indication that the Al_2O_3 film is exhausted as a dopant source as a result of it being ablated from the wafer surface after the initial thermal cycles.

However, independent of the pulse overlap or pulse energy, annealing in either forming gas, or on a hotplate, reduced recombination to equal levels for all but one parameter set. For the Al_2O_3/SiN stack, 90 % pulse overlap (the maximum number of melt cycles) resulted in j_0 > 100,000 fA cm^{-2} for all pulse energies, which could not be recovered by annealing. For the Al_2O_3 single layer, the optimal hot plate annealing temperature was 250 °C, while the lowest recombination for the Al_2O_3/SiN stack was measured following hot plate annealing at 350 °C. From the Al_2O_3 single layer post-annealing recombination was approximately 5,000 – 7,000 fA cm^{-2} across all pulse energies and overlaps, and 8,000 – 10,000 fA cm^{-2} for doping from the Al_2O_3/SiN stack. The increase in recombination in the presence of the SiN capping layer is consistent with the model of thermal mismatch between the SiN film and the silicon substrate enhancing recombination [21], or from the incorporation of additional impurity elements (e.g. N) that enhance recombination.

Annealing in forming gas provided no advantage over the optimal hot-plate annealing conditions (figure 1, bottom). If hydrogen is indeed key to the recovery of laser damage, a hydrogen-rich atmosphere thus provides no measurable advantage over annealing in ambient conditions where hydrogen is present in the Al_2O_3 and/or SiN films.

For both dielectric configurations, recombination is approximately independent of pulse energy and pulse overlap after annealing. This indicates that the damage that accumulates with an increasing number of melt cycles can be restored to roughly equivalent levels by annealing. The exception is the 90 % pulse overlap with Al_2O_3/SiN, which implies a threshold level of damage that is unrecoverable by annealing. This is evidence that recombination at the annealed Al_2O_3-LD surface may not be dominated by laser-induced damage, instead being the result of the aforementioned Al-O complexes. Nonetheless, it is conclusive that annealing is necessary to minimize recombination at Al_2O_3-LD silicon, but this process is likely to reflect a recovery of dopant-independent laser damage. This is in agreement with previous work that has demonstrated lifetime recovery following annealing of laser damage with or with Al [26,27].

For reference, recombination at metallised, furnace boron-doped p^+ silicon in the range of 100 – 200 Ω/□ rises weakly with sheet resistance from approximately 1,000 – 1,200 fA cm^{-2} [34]. In addition, industrially typical fired aluminum emitters are approximately 800 fA cm^{-2} at 60 Ω/□, although it must be acknowledge that there is a lack of reliable data for this process [35].

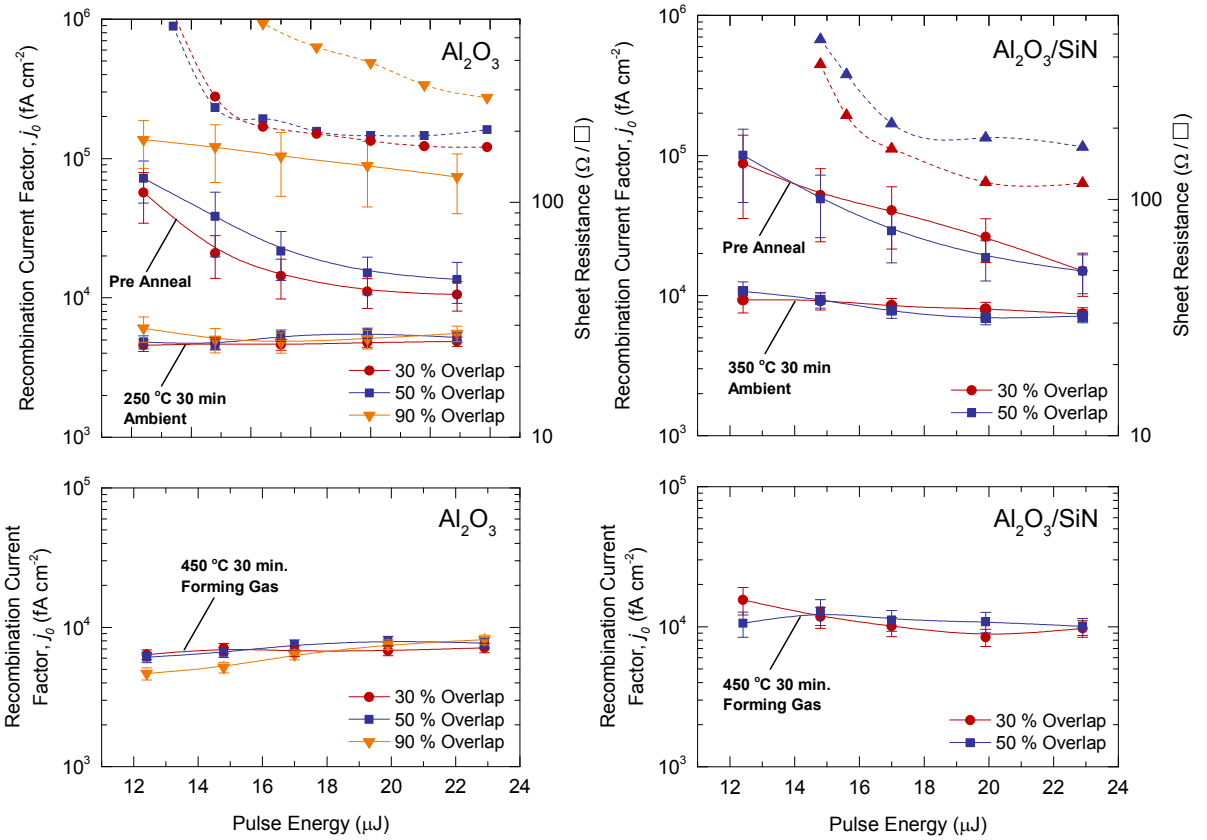

Fig 1. Recombination at Al_2O_3-LD p^+ silicon surface from single-layer Al_2O_3 (left) and an Al_2O_3/SiN stack (right). Recombination is shown at 30, 50 and 90 % pulse overlap before and after the optimal hot plate annealing conditions (top) and after annealing in forming gas (bottom). The dashed lines show the corresponding sheet resistance measured by four-point probe.

3.2. Contact resistivity

When the as-doped surface was contacted with vacuum evaporated Al, contact resistivity exhibited a great deal of scatter, with values ranging between $10^{-2} - 10^{1}$ Ω cm^2 (figure 2, left). A local minimum was measured at 22 μJ for the 30 % pulse overlap, but no clear relationship between energy, overlap and contact resistivity is observed. The resistivity exceeds that of the reference screen-printed and fired Al, which is approximately 3×10^{-3} Ω cm^2. However, sintering at 350 °C for 30 minutes reduced contact resistivity, revealing a strong dependence on pulse energy with minimum values of approximately $2 - 5 \times 10^{-4}$ Ω cm^2 at the highest pulse energies.

The largest reduction in resistivity was measured following a dilute, aqueous, 1 % (by volume) hydrofluoric (HF) acid etch after laser doping but prior to metallisation. This reduction was measured for all laser energies and overlaps, with non-sintered contact resistivity falling into the range of $10^{-4} - 10^{-5}$ Ω cm^2. Similar to recombination, contact resistivity to the etched surface is broadly independent of pulse energy and pulse overlap. It is uncertain why we observe such a large reduction in contact resistivity after etching, but scanning electron microscope images of an Al_2O_3-LD surface revealed an extremely thin surface film that was present following Al_2O_3-LD, but was removed by an HF etch. The necessity of a wet-chemical etch to achieve minimum contact resistivity is an unfortunate complication of the Al_2O_3-LD process. However the energy independence of the contact quality is positive from the perspective of process control, revealing that for the two most critical electronic properties of the Al_2O_3-LD silicon – contact resistivity and recombination – there exists an extremely broad process window that spans the visible energy thresholds of dielectric and substrate ablation. As we will see from the

simulations of section 4, low contact resistivity is crucial to maximise the efficiency of solar cells incorporating rear-surface Al_2O_3-LD silicon.

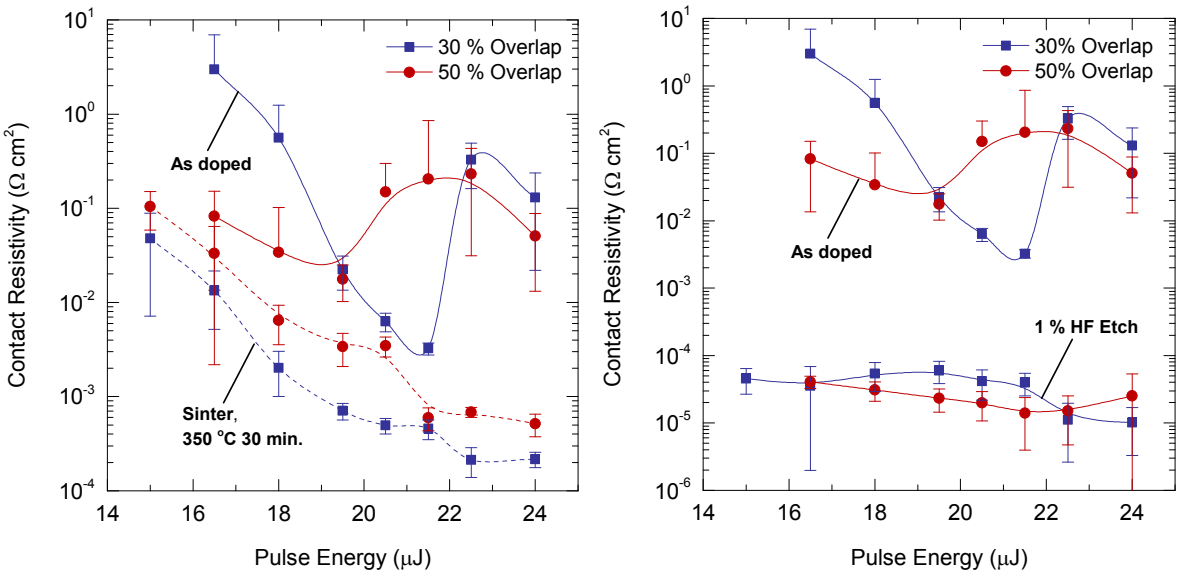

Fig 2. Contact resistivity for an evaporated Al/Al_2O_3 p^+ laser doped silicon interface. Recombination was measured without HF etching, following sintering (left), and after HF etching, but without sintering (right). Following a short HF etch, contact resistivity is approximately uniform across the entire energy range. Note that for legibility the range of the contact resistivity differs between plots.

4. Efficiency potential of PERC-type solar cells incorporating Al_2O_3 laser doping

We have measured recombination at Al_2O_3-LD surfaces, with or without annealing, that exceed that of p^+ silicon of equivalent concentration formed by furnace-doped boron. It is reasonable, therefore, to expect a performance penalty in solar cells incorporating p^+ pulsed laser doping from Al_2O_3. However, we have also measured low contact resistivity to evaporated Al – two orders of magnitude lower than fired Al, for example – that allows the rear contact fraction to be reduced to a small area without compromising the internal resistance of the cell. There will exist an optimal contact geometry that is a compromise between series resistance and effective rear surface recombination. In fabricating the local contact openings with this process, computer controlled laser systems are readily programmed to precisely define arbitrary geometries.

To predict the potential conversion efficiency of PERC cell structures that implement Al_2O_3-LD with an optimized rear surface contact geometry, simulations of two cell structures were performed in *Quokka*. The first device is a PERC cell, which has a uniform, full-area front surface emitter, and screen-printed front and rear contacts. The optical and electronic parameters are industrially typical values, and the reference efficiency is 20.7 %. The UNSW PERL simulation replicates the best device parameters available in the literature for this cell, simulating a reference one-sun efficiency of 24.8 %. Simulations based on these two cell structures provide an indication of the efficiency potential of an industrially relevant cell, in addition to a device with highly optimized optical and electronic properties for which the Al_2O_3-LD contact openings will be a dominant source of recombination. The parameters for both cells have been taken from the forthcoming "Solar Cell Library" [35], available shortly at the PV Lighthouse website [36]. This resource provides Quokka simulation definitions for a range of crystalline silicon cell types using the most up-to-date values available in the literature.

Both simulations were modified to account for rear-surface passivation with a 20 nm Al_2O_3 / 80 nm SiN dielectric stack. Recombination at the non-contacted, undoped rear surface was set to 5 cm/s, which is a conservative value of recombination for this dielectric configuration on p-type silicon [37]. The generation profiles

were modified to account for the rear surface reflection of the Al_2O_3/SiN/pure-Al stack. Changing the rear surface recombination resulted in an initial increase (all other parameters held constant) in device efficiency for both cells, as neither structure originally incorporated such effective rear surface passivation‡. Therefore, these simulations capture both the advantage of reduced non-contacted rear surface recombination provided by Al_2O_3/SiN passivation, and the disadvantage of increased recombination at the Al_2O_3 p^+ doped contacts.

The contact openings were defined as circular, with a diameter of 20 µm and a contact resistivity equal to $\rho_c = 10^{-4}$ Ω cm^2, a conservative upper limit on the resistivity measured for the HF etched Al_2O_3-LD surfaces. Initial simulations demonstrated that point-contacts, arranged in an equidistant square matrix, reached higher efficiencies than line contacts, and the results presented here are restricted to a point contact geometry. The rear surface contact fraction was varied by dependently sweeping the contact pitch in the x and y axis, while the recombination current factor, j_0, was independently varied. The output of these simulations demonstrate the efficiency potential for each combination of contact fraction and recombination (figure 3).

The simulations demonstrate that with low contact resistivity, the rear surface contact fraction can be reduced to less than 1 %, which mitigates the total level of rear surface recombination. For contact recombination at j_0 = 10,000 fA cm^{-2}, the industrial PERC cell has a simulated efficiency of 20.9 %, while the PERL cell can exceed 24 % with an optimised rear contact geometry. It is notable that the combination of laser doping and metal evaporation facilitates a point contact, small feature geometry that allows the PERC cell to exceed the reference level of performance where the rear contacts are line-shaped with fired Al. This despite an increase in contact recombination of approximately 1 order of magnitude relative to screen printed and fired Al.

5. Conclusions

In this work we have characterised recombination and contact resistivity of Al_2O_3 laser doped p^+ silicon formed by a range of laser energies and number of melt cycles using a nanosecond pulse length, 532 nm laser. We observe that recombination, before and after annealing, exceeds that of furnace diffused p^+ boron doped silicon of equivalent sheet resistance. Increasing thermal cycles correlates with increasing laser damage, but this damage is equally recovered by low temperature annealing. Following annealing, recombination is between 8,000 – 10,000 fA cm^{-2} when doping from an Al_2O_3/SiN dielectric stack, and between 5,000 – 7,000 fA cm^{-2} when using a single layer Al_2O_3 precursor. Low resistivity contact requires a short dilute HF etch, following which contact resistance is in the range of $10^{-4} - 10^{-5}$ Ω cm^2 when contacted with evaporated aluminium. Therefore, following annealing and a dilute HF etch, both pulse energy and pulse overlap have a negligible influence on recombination and contact resistivity, which reveals a broad process window.

For PERC cells with local Al_2O_3 laser doped rear contacts, an optimal geometry can be found that minimises effective rear surface recombination while avoiding excessive series resistance. So configured, we see that cell efficiencies can approach 21 % for an industrially typical PERC cell, while the efficiency can exceed 24 % when implemented into a high efficiency locally doped and contacted PERC cell, in this case represented by the UNSW PERL cell.

The primary conclusion is that the reduction in cell efficiency is less than may be initially expected given values of contact j_0 of up to 10,000 fA cm^{-2}. In particular, efficiencies in excess of 24 % can be theoretically achieved by an otherwise highly optimised cell structure. These structures are readily achieved, as computer controlled laser systems can process arbitrary contact geometries at high speed. Al_2O_3 laser doping is therefore compatible with high efficiency PERC-type solar cells.

‡ For example, the surface recombination velocity of the passivated, undoped rear surface of the UNSW PERL cell is estimated at approximately 15 cm s^{-1} at $\Delta n = 1 \times 10^{15}$ cm^{-3} using the parameterisation in [35].

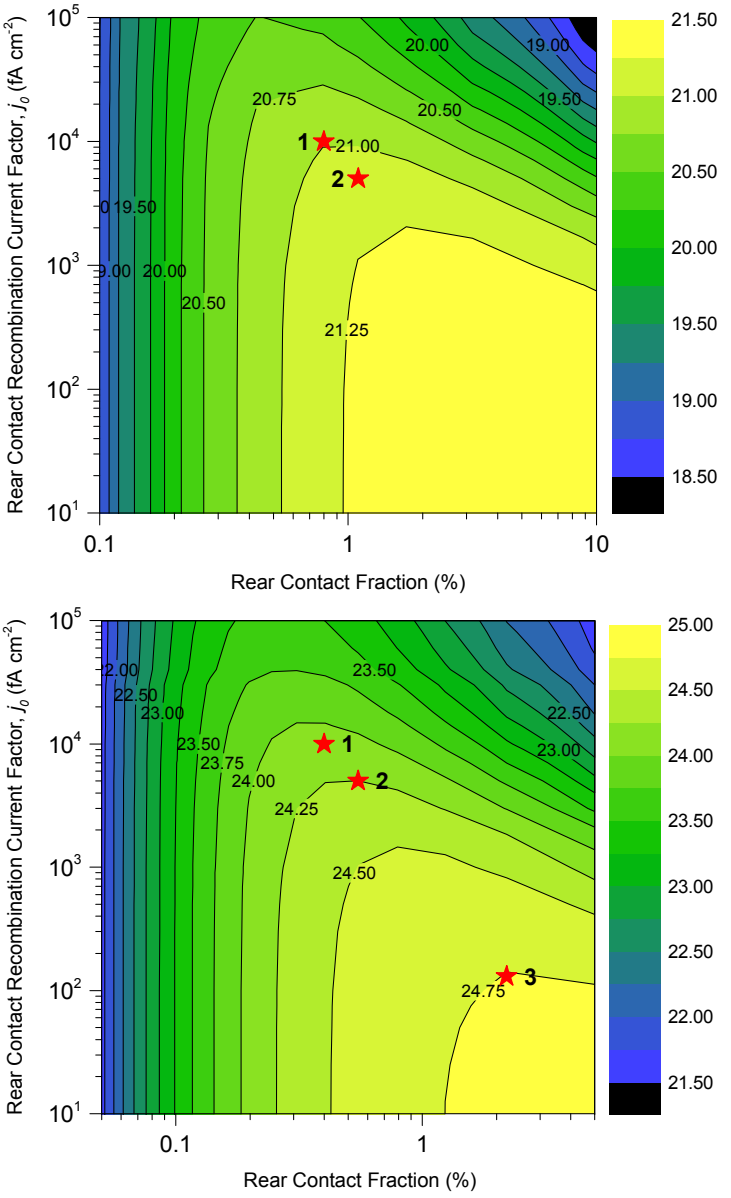

Fig 3. Simulated one-sun efficiency for point contacted industrial PERC (left) and UNSW PERL cell (right) incorporating rear surface passivation with Al_2O_3/SiN and Al_2O_3-LD rear contact openings. Rear contact resistivity is 10^{-4} Ω cm^2. The pentagrams locate the peak efficiency for rear contact recombination, j_0, of (1) j_0 = 10,000 fA cm^{-2}, the post-anneal recombination for Al_2O_3/SiN doping; (2) j_0 = 5,000 fA cm^{-2}, the post-anneal recombination for Al_2O_3 doping; and for the PERL cell (3) the original (non-laser doped) contact recombination where $j_{0,PERL}$ = 130 fA cm^{-2}. Note different efficiency scales for each plot.

Acknowledgements

This work was supported by the Australian Government through the Australian Renewable Energy Agency (Project number 3-GER002). Responsibility for the views, information or advice expressed herein is not accepted by the Australian Government.

References

[1] Fairfield JM, Schwuttke GH. Silicon diodes made by laser irradiation. Solid-State Electronics 1968;11:1175–IN6.
[2] Wenham SR, Green MA. Self aligning method for forming a selective emitter and metallization in a solar cell. US Patent 6,429,037, 2002.
[3] Tjahjono BS, Guo JH, Hameiri Z, Mai L, Sugianto A, Wang S, et al. High efficiency solar cell structures through the use of laser doping. Proceedings of the 22nd European Photovoltaic Solar Energy Conference, 2007, p. 3–7.
[4] Steinhauser B, Jäger U, Benick J, Hermle M. PassDop rear side passivation based on Al 2 O 3/a-SiC x: B stacks for p-type PERL solar cells. Solar Energy Materials and Solar Cells 2014;131:129–33.
[5] Suwito D, Jager U, Benick J, Janz S, Hermle M, Glunz SW. Industrially Feasible Rear Passivation and Contacting Scheme for High-Efficiency n-Type Solar Cells Yielding a of 700 mV. Electron Devices, IEEE Transactions on 2010;57:2032–6.
[6] Dahlinger M, Bazer-Bachi B, Röder TC, Köhler JR, Zapf-Gottwick R, Werner JH. 22.0% Efficient Laser Doped back Contact Solar Cells. Energy Procedia 2013;38:250–3.
[7] Gall S, Vibert J, Pirot M, Lerat J-F, Emeraud T, Le Quang N, et al. Comparison of picosecond laser sources for SiNx ablation with subsequent nickel silicide formation by excimer laser annealing (ELA) for high efficiency silicon solar cells. SPIE Solar Energy+ Technology, International Society for Optics and Photonics; 2013, p. 882609–882609.
[8] Paviet-Salomon B, Gall S, Monna R, Manuel S, Slaoui A. Experimental and analytical study of saturation current density of laser-doped phosphorus emitters for silicon solar cells. Solar Energy Materials and Solar Cells 2011;95:2536–9.
[9] Hallam B, Wenham S, Sugianto A, Mai L, Chong CM, Edwards M, et al. Record large-area p-type CZ production cell efficiency of 19.3% based on LDSE technology. Photovoltaics, IEEE Journal of 2011;1:43–8.
[10].Hoex B, Schmidt J, Pohl P, Van de Sanden MCM, Kessels WMM. Silicon surface passivation by atomic layer deposited Al2O3. Journal of Applied Physics 2008;104:044903.
[11] Martín I, Colina M, Coll A, López G, Ortega P, Orpella A, et al. c-Si solar cells based on laser-processed dielectric films. Energy Procedia 2014;55:255–64.
[12] Fell A, Franklin E, Walter D, Suh D, Weber K. Laser doping from Al2O3 layers. 27th European Photovoltaic Solar Energy Conference, 2012, p. 706–8.
[13] Ortega P, Martín I, Lopez G, Colina M, Orpella A, Voz C, et al. p-type c-Si solar cells based on rear side laser processing of Al 2 O 3/SiC x stacks. Solar Energy Materials and Solar Cells 2012;106:80–3.
[14] Cornagliotti E, Tous L, Uruena A, Rothschild A, Russell R, Lu V, et al. Integration of spatial ALD aluminum oxide for rear side passivation of p-type PERC/PERL solar cells. 28th European Photovoltaic Solar Energy Conference and Exhibition-EUPVSEC, 2013, p. 976–81.
[15] Harder N-P, Larionova Y, Brendel R. Al+-doping of Si by laser ablation of Al2O3/SiN passivation. Physica Status Solidi (a) 2013;210:1871–3.
[16] Kane D, Swanson R. Measurement of the emitter saturation current by a contactless photoconductivity decay method. IEEE photovoltaic specialists conference. 18, 1985, p. 578–83.
[17] Mäckel H, Varner K. On the determination of the emitter saturation current density from lifetime measurements of silicon devices. Progress in Photovoltaics: Research and Applications 2013;21:850–66.
[18] Thomson AF, Hameiri Z, Grant NE, Price CJ, Di Y, Spurgin J. Uncertainty in Photoconductance Measurements of the Emitter Saturation Current. Photovoltaics, IEEE Journal of 2013;3:1200–7.
[19] Min B, Dastgheib-Shirazi A, Altermatt PP, Kurz H. Accurate determination of the emitter saturation current density for industrial P-diffused emitters, Amsterdam, Netherlands: n.d., p. 463–6.
[20] Fischer B. Loss analysis of crystalline silicon solar cells using photoconductance and quantum efficiency measurements. University of Konstanz, 2003.
[21] Hameiri Z, Puzzer T, Mai L, Sproul AB, Wenham SR. Laser induced defects in laser doped solar cells. Progress in Photovoltaics: Research and Applications 2011;19:391–405.
[22] Sugianto A, Tjahjono BS, Guo JH, Wenham SR. Impact of laser induced defects on the performance of solar cells using localised laser doped regions beneath the metal contacts. Proc. 22nd Eur. Photovoltaic Solar Energy Conf, 2007, p. 1759–62.
[23] Marchand RL, Sah C-T. Study of thermally induced deep levels in Al doped Si. Journal of Applied Physics 1977;48:336–41.
[24] Rosenits P, Roth T, Glunz SW, Beljakowa S. Determining the defect parameters of the deep aluminum-related defect center in silicon. Applied Physics Letters 2007;91:122109.
[25] Bock R, Altermatt PP, Schmidt J, Brendel R. Formation of aluminum–oxygen complexes in highly aluminum-doped silicon. Semiconductor Science and Technology 2010;25:105007.
[26] Hallam B, Sugianto A, Mai L, Xu G, Chan C, Abbott M, et al. Hydrogen passivation of laser-induced defects for silicon solar cells. Photovoltaic Specialist Conference (PVSC), 2014 IEEE 40th, IEEE; 2014, p. 2476–80.
[27] Ametowobla M, Bilger G, Köhler JR, Werner JH. Laser induced lifetime degradation in p-type crystalline silicon. Journal of Applied Physics 2012;111:114515.
[28] Zhao J, Wang A, Green MA. 24.5% efficiency PERT silicon solar cells on SEH MCZ substrates and cell performance on other SEH CZ and FZ substrates. Solar Energy Materials and Solar Cells 2001;66:27–36.
[29] Schmidt J, Kerr M, Cuevas A. Surface passivation of silicon solar cells using plasma-enhanced chemical-vapour-deposited SiN films and thin thermal SiO2/plasma SiN stacks. Semiconductor Science and Technology 2001;16:164.
[30] Fell A. A free and fast three-dimensional/two-dimensional solar cell simulator featuring conductive boundary and quasi-neutrality approximations. Electron Devices, IEEE Transactions on 2013;60:733–8.

[31] Fell A, Walter D, Kluska S, Franklin E, Weber K. Determination of injection dependent recombination properties of locally processed surface regions. Energy Procedia 2013;38:22–31.
[32] Cuevas A, Yan D. Misconceptions and misnomers in solar cells. Photovoltaics, IEEE Journal of 2013;3:916–23.
[33] Schroder DK. Semiconductor material and device characterization. Hoboken, New Jersey: John Wiley & Sons; 2006.
[34] Franklin E, Fong K, McIntosh K, Fell A, Blakers A, Kho T, et al. Design, fabrication and characterisation of a 24.4% efficient interdigitated back contact solar cell. Progress in Photovoltaics: Research and Applications 2014.
[35] Fell A, McIntosh, Keith R. Input Parameters for the Simulation of Silicon Solar Cells in 2014. Photovoltaics, IEEE Journal of 2015.
[36] PV Lighthouse n.d. www.pvlighthouse.com.au.
[37] Werner F, Veith B, Tiba V, Poodt P, Roozeboom F, Brendel R, et al. Very low surface recombination velocities on p-and n-type c-Si by ultrafast spatial atomic layer deposition of aluminum oxide. Applied Physics Letters 2010;97:162103–162103.